Amplitude Modulation to Phase Modulation Conversion in Photonic Bandpass Sampling Link

Shanhong Guan, Feifei Yin, Yue Zhou, Kun Xu, and Yitang Dai

***Abstract*—The photonic bandpass sampling has been proved to be potential in multi-carrier communication, frequency-agile coherent radar, compressive sensing, etc. It supports the direct down-conversion of multi-carrier signals using a low-speed analog-to-digital converter (ADC). We observed the distortion resulted from amplitude-modulation to phase-modulation (AM-PM) conversion caused by the saturated photo-detector in the photonic bandpass sampling link. The nonlinearity caused by the AM-PM conversion is theoretically analyzed, which is the 2nd harmonic distortion and has a phase difference of 90 degrees with the fundamental signal. Due to the AM-PM conversion, the 2nd harmonic distortion occurs even the Mach-Zehnder modulator (MZM) is quadrature biased in the photonic bandpass sampling link. Two comparative experiments were conducted to test the nonlinearity. When the MZM works at different bias points, the phase of the 2nd harmonic distortion will be different. In addition, we also compared the differences in 2nd harmonic distortion between standard continuous wave photonic links and photonic bandpass sampling links.**

***Index Terms*—Fiber optics links, photonic bandpass sampling.**

I. Introduction

TO MEET the ever-increasing demand for data capacity, broadband communication systems that support high data rates are being actively investigated. In recent years, commercial modulators and detectors have enabled radio over fiber (RoF) links to handle extremely high instantaneous bandwidths [1]. However, according to the Nyquist theory, it is difficult to digitize the received signal directly after the detector. In commercial or military software defined radios (SDRs), for example, it is urgent to communicate simultaneously with many radios under different radio frequency (RF) bands. In order to digitalize the multi-carrier RF signal, a wideband analog-to-digital converter (ADC) can be used, with usually too high sampling rate if the Nyquist sampling theorem is satisfied. The back-end ADC requires a high sampling rate, posing a challenge for the ADC. Bandpass sampling is currently considered to be a promising alternative technique, which supports direct down-conversion of multi-carrier signals instead of traditional multiple down-conversion [2].

Recently, for the rapidly improved performance of femtosecond lasers, photonic bandpass sampling based on the femtosecond lasers support direct sampling of ultra-wideband, multi-band, multi-carrier radio frequency signals from DC to tens of GHz without down-conversion, effectively reducing the amount of subsequent sample data storage and processing [3]–[5]. The photonic bandpass sampling link has shown performance that rivals that of the standard continuous wave (CW) architecture. The front-end photonic bandpass sampling overcomes the back-end high sampling rate and multilevel down-conversion requirement. It has found more and more applications in high-performance radars[6], compressive sensing [7], [8], and multi-carrier communication [9], [10], etc. As with the traditional CW-based analog photonic link, the sampled radio frequencies are also distorted by all kinds of nonlinearities arising from the Mach-Zehnder modulator (MZM) and other nonlinear devices due to the nonlinear electronics-optics-electronics (E/O/E) conversion in the photonic bandpass sampling link. To improve the link's spurious-free dynamic range (SFDR) and fidelity, all the generated nonlinear distortions need to be well eliminated. In particular, both the target signals and derived nonlinear distortions are sampled and frequency-folded within the first Nyquist zone in the bandpass sampling link. In our previous work [11], all of the 3rd-order nonlinearities arising from the MZM were well compensated except the significant 2nd-order nonlinear spurs generating by the photo-detector (PD).

In most situations, distortions caused by PD are not under consideration since the PD shows un-conspicuous nonlinearity in the non-saturated linear range. However, PD is easy to get saturated and causes nonlinearity when the incident beam is a pulsed light source because the peak power of the pulsed light source is much higher than that of the CW light source under the same average optical power [12]. It has been demonstrated that the phase of the directly detected electrical signal changes as a function of the applied optical energy for the un-modulated optical pulse trains due to the PD saturation effect [13]. The saturated PD converts optical amplitude noise to microwave phase retardation, thereby worsening the extracted microwave signal phase noise [14].

In this paper, we find that the amplitude modulation will also convert into the phase modulation in the bandpass sampling RF photonic links when PD operated under saturated input conditions. The converted phase modulation results in the significant 2nd harmonic distortion, which can be observed even if the MZM

Manuscript received June 30, 2021; revised July 14, 2021; accepted July 15, 2021. Date of publication July 21, 2021; date of current version August 5, 2021. This work was supported in part by the National Key Research and Development Program of China under Grant 2018YFA0701902, in part by the National Natural Science Foundation of China under Grants 62071055, 62001043, and 61901428, and in part by the ZTE Industry-Academia-Research Cooperation Funds. *(Corresponding author: Yitang Dai.)*

The authors are with the State Key Laboratory of Information Photonics & Optical Communications, Beijing University of Posts and Telecommunications, Beijing 100876, China (e-mail: guansh@bupt.edu.cn; yinfeifei@bupt.edu.cn; yuezhou@bupt.edu.cn; xukun@bupt.edu.cn; ytdai@bupt.edu.cn).

Digital Object Identifier 10.1109/JPHOT.2021.3098311

is quadrature biased. It is well known that the other kind of 2nd harmonic distortion caused by the MZM will generate only when the operating point drifts away from the quadrature bias point. We study the characteristics of the distortion caused by AM-PM conversion in the photonic bandpass sampling system, which is of great significance for suppressing this nonlinearity and improving the performance of the photonic bandpass sampling system. In our previous work [11], we achieved the suppression of the third-order nonlinear spurs generated by the modulator transfer function through digital compensation. We find that the nonlinearity caused by AM-PM conversion is not the same as the nonlinearity caused by the MZM, and cannot be suppressed in the same way. Therefore, we study the characteristics of nonlinear spurs caused by AM-PM conversion in this paper. The 2nd harmonic distortion resulted from AM-PM conversion shows a phase difference from that of the fundamental signal, which is quite different from the one caused by the nonlinearity of the MZM. We find that the frequency of the nonlinear distortion caused by AM-PM conversion is twice that of the fundamental signal, and secondly, there is a fixed phase difference between the nonlinear distortion and the frequency-multiplied fundamental signal. Two comparison experiments are conducted to examine the phase difference of the two kinds of nonlinearities. In addition, we also compare the phase difference between the 2nd order distortion and the frequency multiplied fundamental signal in both CW photonic links and photonic bandpass sampling links under the same fundamental signal and 2nd harmonic distortion.

II. Principle

Since the pulse width of the light source used in the photonic bandpass sampling link is of the order of magnitude femtosecond, its instantaneous power is far higher than the CW laser at the same average power. The ultra-high instantaneous optical power results in PDs being easily to get saturated during the photoelectric conversion process. Both the high density of photo-carriers and the limited carrier mobility in the PD will reduce the response time. It will further lead to instability of the pulse sequence in amplitude and phase, which converses the amplitude jitter of the recovered microwave signal into phase retardation. In the previous works, the other researchers have studied the relationship between the phase change of the output signal of the PD and the incident optical power of the pulsed light source [13]. In this part, the nonlinear distortion introduced by AM-PM conversion is theoretically analyzed in the photonic bandpass sampling link.

In the photonic bandpass sampling link, it is assumed that the repetition frequency of optical pulse generated by the mode-locked laser is f_{O} and each pulse is described by its normalized intensity profile, $q(t)$, where $\int q(t)\mathrm{d}t = 1$, then the normalized pulse amplitude can be expressed as

$$I_O = \sum_k q\left(t - k/f_O\right). \tag{1}$$

After the MZM, the pulse sequence is modulated by a signal of amplitude $a(t)$. As have been proven in [11], the modulation process is equivalent to bandpass sampling the modulated RF signal. The modulated signal is

$$\begin{aligned} I_M &= a\left(t\right)\sum_k q\left(t - k/f_{\mathrm{O}}\right) \\ &\approx \sum_k a\left(k/f_{\mathrm{O}}\right) q\left(t - k/f_{\mathrm{O}}\right). \end{aligned} \tag{2}$$

We denoted $a(k/f_{\mathrm{O}})$ as a_k, which is the amplitude of the direct discrete sample of the input with a sampling rate of f_{O}. The approximation stands when the femtosecond pulse approaches an impulse function. In the modulation process, the microwave signal $a(t)$ is down-converted by the optical pulse train and its carrier frequency is greatly decreased. Assuming that the frequency of the $a(t)$ is f_s, the frequency of the down-converted intermediate frequency (IF) signal is

$$f_{IF} = f_s - Nf_O, |f_{IF}| < f_O/2. \tag{3}$$

Theoretically, the modulated signal $a(t)$ is mixed with the pulse sequence and generates multiple frequency components in the frequency domain, where the intermediate frequency signal is located within the first Nyquist zone. After the PD, the electrical signal is

$$v_{\mathrm{PD}} = \sum_k a_k q_{a_k}\left(t - k/f_{\mathrm{O}} - \tau\left(a_k\right)\right). \tag{4}$$

We consider the nonlinear saturation effect of PD, where the output pulse width, q_{a_k},and the time delay, $\tau(a_k)$, are both disturbed by the energy of each optical pulse, a_k. According to [13], the PD moves to a saturated regime under high incident optical power. The resulting electrical pulses move later in time as the optical power is increased. After filtering, the IF signal located in the first Nyquist zone can be expressed as the following form:

$$\begin{aligned} v_{\mathrm{IF}} &= \sum_k a\left(k/f_{\mathrm{O}} + \tau\left(a_k\right) - \tau\left(a_k\right)\right) q_{a_k}\left(t - k/f_{\mathrm{O}} - \tau\left(a_k\right)\right) \\ &\approx a\left(t - \tau\left(a\right)\right)\sum_k q_{a_k}\left(t - k/f_{\mathrm{O}} - \tau\left(a_k\right)\right) \\ &\to a\left(t - \tau\left(a\right)\right) \end{aligned} \tag{5}$$

The approximation in Eq. (5) stands when the duration of electronic pulse is much smaller than the period of IF tone. In [13], it has been proved that the pulse centroid motion during PD saturation fits a linear shift. Approximately, we can consider $\tau(a) = \gamma a$, that is, the time jitter is proportional to the optical power, where γ is the saturation coefficient related to PD. From Eq. (5), we can conclude that the output of PD when the modulated signal is $x(t)$ can generally expressed as

$$y = x\left(t - \gamma x\left(t\right)\right). \tag{6}$$

Supposing $x(t) = \frac{1}{2\pi}\int X(\omega)e^{i\omega t}d\omega$, then

$$\begin{aligned} y &= \frac{1}{2\pi}\int X\left(\omega\right)e^{i\omega\left(t-\gamma x\left(t\right)\right)}d\omega \\ &\approx \frac{1}{2\pi}\int \left(1 - i\omega\gamma x\left(t\right)\right)X\left(\omega\right)e^{i\omega t}d\omega \\ &= x\left(t\right)\left(1 + \gamma x'\left(t\right)\right). \end{aligned} \tag{7}$$

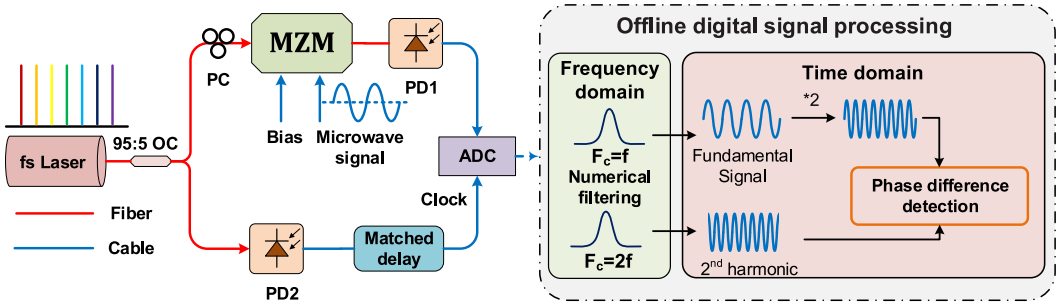

Fig. 1. Schematic diagram of the photonic bandpass sampling RF link and offline digital signal processing.

In Eq. (7), the approximation stands under small modulation depth γ. In the photonic bandpass sampling link, the transfer function for the optical intensity of the MZM operating at quadrature bias point is $y = \sin \beta x$, where β is the modulation depth. If the RF signal is $\cos(\Omega t)$, since the modulation depth is small, the modulated signal after the quadrature-biased MZM can be approximated as $\beta \cos(\Omega t)$. According to Eq. (7) the input of the ADC is

$$\begin{aligned} y &= x(t)\left(1+\gamma x'(t)\right) \\ &= \beta\cos(\Omega t)\left(1-\beta\gamma\Omega\sin(\Omega t)\right) \\ &= \beta\cos(\Omega t)+\frac{\beta^2\gamma}{2}\Omega\cos\left(2\Omega t+\frac{\pi}{2}\right). \end{aligned} \tag{8}$$

It can be seen from the theoretical deduction that when the AM-PM conversion is introduced by the saturated PD in the photonic bandpass sampling link, there will be 2nd harmonic distortion generated even if the modulator is quadrature biased. Since the frequency of the fundamental signal is different from that of the 2nd harmonic distortion, it is not feasible to compare their phase directly. Therefore, we compare the phase of the frequency multiplied fundamental signal with that of the 2nd harmonic distortion. The detected 2nd harmonic distortion has a phase difference of 90 degrees from the frequency multiplied fundamental signal.

In the traditional CW photonic links, the 2nd harmonic distortion will only occur when the MZM operating point deviates from the quadrature bias point. In order to compare with the 2nd harmonic distortion in the photonic bandpass sampling link, the transfer function of the CW photonic link deviating from the quadrature bias point under a small modulation depth β is expanded as follows

$$\begin{aligned} y &= \sin(\beta x+\varphi) \\ &\approx \beta x\cos\varphi+\left(1-\frac{\beta^2x^2}{2}\right)\sin\varphi \\ &= \sin\varphi-\frac{\beta^2}{4}\sin\varphi+\beta\cos\varphi\cos(\Omega t)+\frac{\beta^2}{4}\sin\varphi\cos(2\Omega t), \end{aligned} \tag{9}$$

where φ is the angle of the MZM operating point offset from the quadrature bias point. We can see that the 2nd harmonic distortion, which is caused by the MZM, is only generated when the MZM operating point deviates from the quadrature bias point. In addition, the phase of the 2nd harmonic distortion is the same as that of the frequency multiplied fundamental signal, which is different from the one caused by the statured PD in the photonic bandpass sampling link.

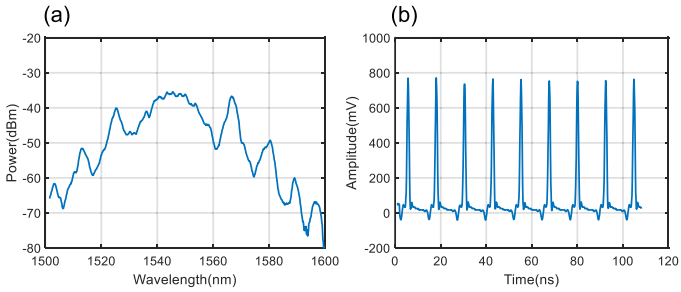

Fig. 2. (a) The optical spectra and (b) pulse waveform of the mode-locked laser.

III. Experiment and Results

The classical photonic bandpass sampling link employing the optical pulse train is shown in Fig. 1. In our experiment, the optical pulse train, which is generated from a homemade passive mode-locked Er-fiber laser, has a fundamental repetition rate of 78.42 MHz and full width at half maximum (FWHM) pulse duration of 401.7 fs. The laser resonant cavity is composed of two parts: a free space optical path and a section of single-mode fiber. The total length of the cavity is about 2.56 m. All the optical fibers are positive dispersion single-mode fibers. When the pump power of the 980 nm laser is 200 mW, the output power of the mode-locked laser is about 3.8 mW. The optical spectra and pulse waveform of the mode-locked laser are shown in Fig. 2(a) and 2(b), respectively. After the optical coupler (OC), approximately 5% of the femtosecond pulse train is detected directly by the low-speed PD2 (New Focus, Model 1611) to synchronize the ADC (ADlink PCIE-9852). The other 95% is used in the optical sampling of the RF signal after the polarization controller (PC). The input 10 MHz microwave signal is modulated on the pulse train by the MZM (EOSpace, 20 GHz) of which the operation point is fixed by a homemade dither-free bias controller. The insertion loss of the MZM is about 4 dB. Both the input and the output fibers are polarization maintaining. The half-wave voltage at 1 GHz is about 5V. Then, the modulated optical

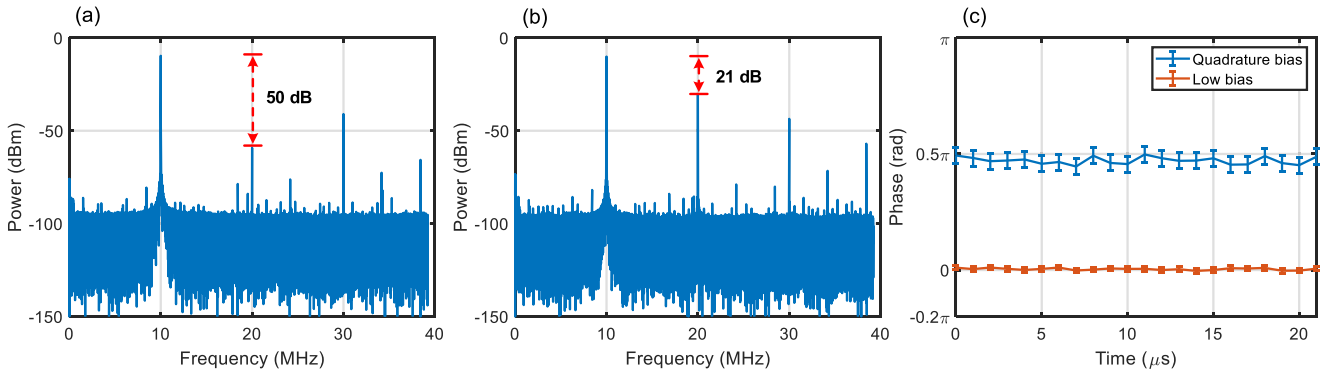

Fig. 3. The RF spectrums of photonic bandpass sampling link with MZM operating at (a) quadrature bias point and (b) low bias point. (c) The phase difference of fundamental and 2nd harmonic distortion with MZM operating at quadrature bias point (blue line) and low bias point (red line).

signal is sent to a homemade PD1 (6 GHz bandwidth with a responsivity of 0.9 A/W). The maximum input optical power of the PD is about 10dBm. The power of the input RF signal is fixed at 4 dBm at the MZM. The average powers of the light-wave hitting on the PD1 are 3 dBm and 0 dBm, when the MZM are quadrature biased and low biased, respectively. We used a 200 MHz bandwidth ADC to digitize the PD output signal. In the digital domain, offline digital signal processing (DSP) is introduced to identify the phase retardation of the harmonic distortion. Firstly, two narrowband numerical filters are introduced to extract the fundamental signal and 2nd harmonic distortion from the received digitized signal, respectively. Then, we compare the phase difference between the 2nd harmonic distortion and frequency multiplied fundamental signal, as shown in Fig. 1.

Two comparison experiments are conducted to examine the phase retardation of the 2nd harmonic distortion by driving the MZM at quadrature and low bias points, respectively. The received RF spectrums with different operating points are shown in Fig. 3(a) and (b). We can observe the considerable nonlinear distortions around the fundamental signal within the first Nyquist zone. The corresponding phase difference between fundamental and 2nd harmonic distortion can be observed in Fig. 3(c). When the MZM is operating at the low bias point, the significant 2nd harmonic distortion will generate from the MZM and dominate the nonlinearity, the power ratio between fundamental and 2nd harmonic distortion is 21 dB, as shown in Fig. 3(b). As is known that the 2nd harmonic distortion can be ignored when the MZM is quadrature biased in the CW analog photonic links. However, in the photonic bandpass sampling link, the 2nd harmonic distortion still distorts the fundamental signal even if the MZM is quadrature biased, as shown in Fig. 3(a). Therefore, the AM-PM conversion nonlinearity due to the saturated PD dominates the 2nd-order distortion when the photonic bandpass sampling link is quadrature biased. The two types of nonlinearity, i.e., phase modulation conversation distortion caused by the saturated PD and amplitude modulation distortion caused by the nonlinearity of MZM operating at the low bias point, dominate the 2nd harmonic distortion of the photonic bandpass sampling link operating at quadrature and low biased point, respectively. When the MZM is operating at the low bias point, the phase difference between the fundamental signal and the 2nd harmonic distortion is close to 0 in the photonic bandpass sampling link, which is the same as that of the CW photonic link shown in Fig. 3(c). However, when the MZM is quadrature biased, the 2nd harmonic distortion shows a phase difference of $\pi/2$ from the frequency multiplied fundamental signal. It indicates that the 2nd harmonic distortion caused by phase distortion conversion will have $\pi/2$ phase retardation, which is different from the one caused by amplitude-dependent nonlinearity.

We noticed that when the MZM operating point is offset from the quadrature bias point, the 2nd-order spurs caused by the nonlinearity of the MZM will be generated. The distortion caused by MZM is mixed with the one caused by saturated PD and cause errors in the final measured phase results. When the MZM operating point is drifting from the quadrature bias point, the power ratio of the 2nd-order distortion generated by the nonlinearity of the modulator to the fundamental signal is $[\frac{J_2(\beta)}{2J_1(\beta)}\tan\varphi]^2$, where $J_n(*)$ is the n-th order Bessel function of the first kind. β is the modulation depth, and φ is the angle of the MZM operating point deviating from the quadrature bias point. The bias phase stability of the bias controller working at the quadrature bias point is ± 1.0 degree. The phase error caused by the drifting of the MZM bias point is about 0.034π. In the low bias bandpass sampling link, the 2nd-order distortion caused by saturated PD is related to the power of the fundamental signal. When the power of the fundamental signal is the same, the 2nd-order distortion caused by the nonlinearity of the modulator is about 30 dB higher than that caused by the saturated PD, and the corresponding phase error between fundamental signal and the 2nd-order distortion is about 0.01π.

In the photonic bandpass sampling link, when the 2nd harmonic distortion is minimal, the MZM is exactly quadrature biased. We compare the 2nd harmonic distortion in both the CW photonic link and the photonic bandpass sampling link. The photonic bandpass sampling link that operating at the quadrature bias point is also demonstrated as the reference. In Fig. 1, the femtosecond laser is replaced with a CW laser in the CW photonic link, and the synchronized clock of the ADC is canceled. Under the same input RF signal, by changing the optical power of the laser and the bias point of the MZM in the CW photonic link, the fundamental signal and the 2nd harmonic distortion are set to equal with that of the photonic bandpass sampling

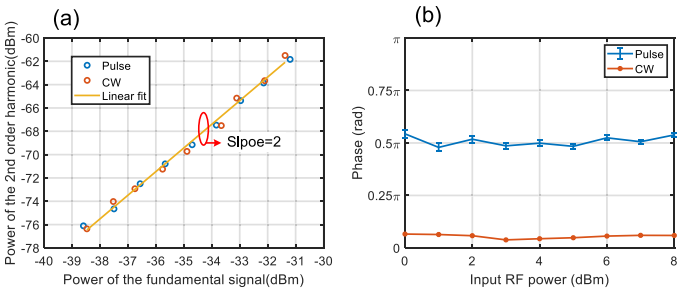

Fig. 4. (a) The fundamental signal and the 2nd harmonic distortion in the CW photonic link and photonic bandpass sampling link under the same RF input. (b) The phase difference of the CW photonic link and the photonic bandpass sampling link with different input RF power.

link. Under such conditions, the MZM is operating at the low bias point in the CW photonic link. When the input RF signal power varies from 0 dBm to 8 dBm, the fundamental signal and the 2nd harmonic distortion are recorded as shown in Fig. 4(a). While changing the RF signal, the fundamental signal and the 2nd harmonic distortion in the two links are almost equal. Under this circumstance, we compare the phase difference between the fundamental signal and the 2nd harmonic distortion in the two links. In Fig. 4(b), we can see that when the input RF signal ranging from 0 dBm to 8 dBm, the phase difference is close to 90 degrees in the photonic bandpass sampling link, while the phase difference is close to 0 in the CW photonic link. We also calculated the phase error caused by the drift of the MZM operating point in the pulse bandpass sampling link and marked it in the figure.

When the MZM is quadrature biased in the photonic bandpass sampling link, the amplitude of the 2nd harmonic distortion, which is caused by the AM-PM conversion, is the same as that of the low biased CW photonic link as long as the input RF signal and gain of the two links are the same. However, the 2nd harmonic distortion caused by the AM-PM effect has a phase difference of 90 degrees from that of the fundamental signal. It is different from that of the CW photonic link. Moreover, the nonlinearity caused by AM-PM conversion cannot be eliminated simply by adjusting the MZM operating point and should be suppressed by exploring new methods.

IV. Conclusion

In conclusion, we have theoretically and experimentally demonstrated the harmonic phase change in photonic bandpass sampling RF link with saturated PD. Experiment results show that severe 2nd harmonic distortion caused by the AM-PM conversion can still be observed even if the MZM is quadrature biased. Different from the amplitude-dependent nonlinearity, the AM-PM conversion nonlinearity results in $\pi/2$ phase difference. Compared with the CW photonic link, the amplitude of the 2nd harmonic distortion caused by the AM-PM conversion in the photonic bandpass sampling link is the same as the 2nd harmonic in the low biased CW photonic link under the same input and gain. Although a low-speed system is used to study the nonlinearity caused by AM-PM conversion, these conclusions are also applicable to systems with larger bandwidths. In addition, the nonlinearity caused by the AM-PM conversion has a phase difference of $\pi/2$ from the frequency multiplied fundamental signal, which means the traditional methods of suppressing the 2nd-order nonlinearity caused by MZM may no longer be suitable for the nonlinearity caused by AM-PM conversion. After studying the nonlinear characteristics caused by AM-PM conversion, we can suppress it through appropriate digital compensation techniques in the subsequent work. In particular, the 90 degrees' phase lag compared to the fundamental frequency signal is the key factor in suppressing the nonlinear spurs and it has not been encountered in the previous nonlinearity digital compensation techniques.

References

[1] J. Capmany and D. Novak, "Microwave photonics combines two worlds," *Nature Photon.*, vol. 1, no. 6, pp. 319–330, Jun. 2007.
[2] C.-H. Tseng and S.-C. Chou, "Direct downconversion of multiband RF signals using bandpass sampling," *IEEE Trans. Wireless Commun.*, vol. 5, no. 1, pp. 72–76, Jan. 2006.
[3] A. Khilo *et al.*, "Photonic ADC: Overcoming the bottleneck of electronic jitter," *Opt. Exp.*, vol. 20, no. 4, pp. 4454–4469, Feb. 2012.
[4] H. Kim *et al.*, "Sub-20-Attosecond timing jitter mode-locked fiber lasers," *IEEE J. Sel. Topics Quantum Electron.*, vol. 20, no. 5, pp. 260–267, Sep. 2014.
[5] P. W. Juodawlkis *et al.*, "Optically sampled analog-to-digital converters," *IEEE Trans. Microw. Theory Techn.*, vol. 49, no. 10, pp. 1840–1853, Oct. 2001.
[6] P. Ghelfi *et al.*, "A fully photonics-based coherent radar system," *Nature*, vol. 507, no. 7492, pp. 341–345, Mar. 2014.
[7] M. Fleyer, M. Horowitz, A. Feldtser, and V. Smulakovsky, "Multi-rate synchronous optical undersampling of several bandwidth-limited signals," *Opt. Exp.*, vol. 18, no. 16, pp. 16929–16945, Aug. 2010.
[8] L. Yan *et al.*, "Integrated multifrequency recognition and downconversion based on photonics-assisted compressive sampling," *IEEE Photon. J.*, vol. 4, no. 3, pp. 664–670, Jun. 2012.
[9] M. Cao, J. Li, Y. Dai, F. Yin, and K. Xu, "Bandpass sampling based digital coherent receiver with free-running local oscillator laser for phase-modulated radio-over-fiber links," *Opt. Exp.*, vol. 22, no. 22, pp. 27007–27018, Nov. 2014.
[10] Y. Yang, C. Lim, and A. Nirmalathas, "Multichannel digitized RF-Over-Fiber transmission based on bandpass sampling and FPGA," *IEEE Trans. Microw. Theory Techn.*, vol. 58, no. 11, pp. 3181–3188, Nov. 2010.
[11] Y. Dai *et al.*, "Digital linearization of multi-carrier RF link with photonic bandpass sampling," *Opt. Exp.*, vol. 23, no. 18, pp. 23177–23184, Sep. 2015.
[12] J. A. Taylor *et al.*, "Phase noise in the photodetection of ultrashort optical pulses," in *Proc. IEEE Int. Freq. Control Symp.*, Jun. 2010, pp. 684–688.
[13] M. Currie and I. Vurgaftman, "Microwave phase retardation in saturated ingaas photodetectors," *IEEE Photon. Technol. Lett.*, vol. 18, no. 13, pp. 1433–1435, Jul. 2006.
[14] J. Taylor *et al.*, "Characterization of power-to-phase conversion in high-speed P-I-N photodiodes," *IEEE Photon. J.*, vol. 3, no. 1, pp. 140–151, Feb. 2011.